A three-dimensional regional scale model for tidal stream turbine implementation and impact assessment

Xiaorong Li, Ming Li, Judith Wolf, Alison J. Williams, Charles Badoe, and Ian Masters

Abstract—**This research aims to implement a three-dimensional regional scale numerical model within a region of the Irish Sea (between 52.808˚N and 53.842˚N) that is suitable for turbine array implementation and impact assessment. This research is based on a three-dimensional wave-current-sediment fully coupled oceanographic model (FVCOM), and modifications made by the authors to the current, turbulence and surface wave modules to simulate the potential impact of tidal turbines. The baseline model, i.e. without turbine implementation, is validated extensively against water level measurements at two tide gauges, tidal current data collected at four locations, and wave climate collected by a WaveNet bouy. In the case study, 18 turbines of 15-20 m diameter are modelled individually in the waterway between Anglesey and the Skerries. Results reveal the potential effects of the turbine farm on flow field, turbulence kinetic energy (TKE), bed shear stress and surface waves. Defining the wake edge as flow recovery to 95% of the baseline case, there are slight wake effects for a distance of around 14 times the array width downstream of the device farm. As a result of the high spatial resolution used, local effects of the turbine farm are revealed by the model, such as flow acceleration on both sides of the turbine farm, flow acceleration near the bed in the vicinity of the turbine farm which leads to enhanced bed shear stress, and locally increased TKE.**

Keywords—**Hydrodynamic modelling, large scale modelling, West Anglesey Demonstration Zone, tidal stream turbine arrays.**

I. Introduction

TIDAL stream energy, as a resource of clean renewable energy, has been gaining significant attention due to its predictability and widespread availability. According to [1], a total of 20.6 TWh per year could be extracted from 30 key tidal stream sites in the UK. Since the commencement of the MeyGen project in 2010, the current operational tidal stream energy capacity in the UK is 10 MW with 2 MW under construction. A further 1,000 MW sites are also leased for future development [2].

Alongside the major technology advances made in the last two decades, modelling techniques for device and array design, site evaluation and environmental impact assessment also progressed significantly. For example, tidal turbine simulators used in laboratory experiments advanced from porous discs [3] to scaled turbine prototypes [4]. The size of the prototypes also increased from less than 0.5 m [5] to more than 1 m in diameter [6], drawing closer to the scale of a realistic implementation. Furthermore, experiments are being conducted under comprehensive hydrodynamic conditions, such as the inclusion of surface waves [7].

Due to its high accuracy in resolving flow fields, Computational Fluid Dynamics (CFD) has been a common alternative to physical experiments. At a high computational cost, the geometries of turbines and their motions can be explicitly resolved in a CFD model [8]. The Blade Element Momentum – CFD (BEM-CFD) combined approach, on the other hand, represents turbines with discs and simulates time averaged turbine behaviours, with the impact of turbines on the flow simulated by body force terms added to the momentum equations [9]. More recently, corrections have been made to the BEM-CFD method to capture tip loss effects, and to include considerations for Reynolds number effects and surface roughness [10][11]. Similarly, the Actuator Line – CFD (AL-CFD) method represents rotor blades as rotating lines which exert retarding forces on the passing flow. Because

1654 - Tidal Hydrodynamic Modelling. This work is part of the Selkie project, funded by the European Union's European Regional Development Fund through the Ireland Wales Cooperation programme.

X. Li was a PhD student in the School of Engineering, University of Liverpool, Liverpool, L69 3GQ, UK. She is now a researcher in the Energy and Environment Research Group, College of Engineering, Swansea University, Swansea, SA2 8PP, UK. (e-mail: xiaorong.li@swansea.ac.uk).

M. Li is a senior lecturer in the School of Engineering, University of Liverpool, Liverpool, L69 3GQ, UK. (e-mail: m.li@liverpool.ac.uk).

J. Wolf is a scientist at the National Oceanography Centre, Joseph Proudman Building, 6 Brownlow Street, Liverpool, L3 5DA, UK. (e-mail: jaw@noc.ac.uk).

A. J. Williams is a senior lecturer in the Energy and Environment Research Group, College of Engineering, Swansea University, Swansea, SA2 8PP, UK. (e-mail: alison.j.williams@swansea.ac.uk).

C. Badoe is a researcher in the Energy and Environment Research Group, College of Engineering, Swansea University, Swansea, SA2 8PP, UK. (e-mail: c.e.badoe@swansea.ac.uk).

I. Masters is a professor in the Energy and Environment Research Group, College of Engineering, Swansea University, Swansea, SA2 8PP, UK. (e-mail: i.masters@swansea.ac.uk).

Fig. 1. Location of the Anglesey Coast and the study domain of the model. The Anglesey Coast is depicted by the red box and the study domain is enclosed by the blue lines (open boundaries) and two natural coasts. The inset shows the location of the Skerries.

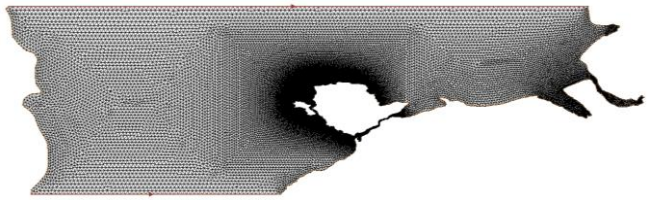

Fig. 2. Mesh of the model. The spatial resolution is 15-20 m in the Sound between the Skerries and mainland Anglesey and 100 m around the Anglesey coast. It increases gradually towards the open boundaries to a resolution of 1600 m.

the actuator lines rotate to a new angle at each computational time step, the AL-CFD method can also resolve time dependent features [12].

For resource characterization and impact assessment, coastal area models are often used. Spatial resolution of these models varies from a few meters [13] to a few kilometres [14]. Hence the geometries of turbines and their motions cannot be explicitly resolved in these models. Instead, turbines and their impact on the flow are often simulated as increased bottom drag or additional body force terms in momentum equations. In the last decade, the application of these models advanced from two-dimensional depth-averaged [15] to three-dimensional implementations [16]. Processes that are adapted in the model to simulate interactions between turbines and their surrounding environment progressed from current [17][18][19][20] to turbulence [19][20], surface waves [21] and sediment transport dynamics [22].

This research aims to implement and validate a three-dimensional regional scale model [20][21] within a region of the Irish Sea (between 52.808°N and 53.842°N) . This validated model is aiming to provide the basis for turbine implementation (within both its native form and CFD derivatives) and impact assessment.

II. METHODOLOGY

A. *Modelling system*

This research is based on a three-dimensional wave-current-sediment fully coupled oceanographic model — the Unstructured Grid Finite Volume Community Ocean Model (FVCOM), and modifications made by the authors to the current, turbulence and surface wave modules to simulate the interactions between tidal turbines and their surrounding environments [19][20].

In the newly developed model, in order to simulate energy extraction which leads to reduced flow rate, an additional body force is added to the momentum equations at the computational cell where individual turbines are allocated [20]. The varying turbine configuration and operation across the water column is represented by a depth-dependent coefficient for the additional body force term. Three turbulence perturbation terms are added to the MY-2.5 turbulence closure to mimic the turbine-induced turbulence generation, dissipation and interference for turbulence length-scale [20]. The built-in function 'OBSTACLE' is used to simulate wave height drop at turbine locations [21]. For the reason of simplicity, the controlling equations of FVCOM and the formulations for turbine parameterization are not included here. For a detailed introduction, one may refer to ref. [20][21].

B. *Study site*

The model domain of this study is enclosed by two natural coasts, the East coast of Ireland and the West coast of the UK, and two open boundaries (blue lines in Fig. 1). Within this area, the Anglesey coast in Northwest Wales (red box in Fig. 1) features high tidal ranges and large current velocities (> 2.5 m/s during spring tide) [23]. This coastal sea region, therefore, is of high potential to be converted into a tidal stream energy extraction site. In fact, this area has been identified as one of the seven sites of interest for tidal current energy exploitation in the UK [24]. Further, the area around the promontory of Holy Island, known as the West Anglesey Tidal Demonstration Zone (Morlais), is planned to host device developers and to provide a maximum of 240MW to the grid [25][26]. In this research, the water between the Skerries (see inset of Figure 1) and mainland Anglesey, where the water depth is approximately 20 to 40 m, is selected to implement a turbine farm comprised of 18 turbines.

C. *Model setup*

The mesh of the model (shown in Fig. 2) is refined to a spatial resolution of 100 m around the Anglesey coast and it is further refined to 15-20 m in the Sound between the Skerries and mainland Anglesey to allow turbines to be presented individually. Mesh size increases gradually towards the open boundaries to a resolution of 1600 m. The bathymetry of the model is extracted from a previous model that covers the West Coast of the United Kingdom [27]. Fig. 3 demonstrates the bathymetry of the model with locations of tidal level, tidal current, surface wave and sediment concentration validation datasets imposed. For a three-dimensional implementation, the water column is divided into 50 sigma layers with identical layer thickness.

The model is driven by tidal elevations obtained from harmonic analysis of 15 tidal constituents (M_2 Q_1 O_1 P_1 S_1 K_1 $2N_2$ MU_2 N_2 NU_2 L_2 T_2 S_2 K_2 M_4) extracted from the High Resolution UK Continental Shelf Model (CS20-15HC3) and

wave conditions provided by the ECMWF 'ERA-Interim' dataset. A time varying uniform wind field based on data measured at the Hilbre Island weather station is used to drive the wave climate. The sediment particle size is specified as D_{50} = 0.22 mm across the entire study domain.

The model is run twice to include a baseline case, i.e. without turbines, and a case incorporating the above-mentioned turbine farm. For the baseline case, the model is run over a month and two days, covering the period from 28/04/2006 00:00:00am to 01/06/2006 00:00:00am. For the case with turbines, the model is run from 17/05/2006 07:00:00am to 20/05/2006 05:00:00am which includes five and a half tidal cycles (Fig. 4) between Spring and Neap tides (the start and end of this period are shown in Fig. 6). During this time period, wave height peaks at 3.62 m at the selected turbine farm location (Fig. 4), representing moderate wave to stormy wave conditions.

Fig. 5 depicts a typical flow pattern based on depth-averaged velocity between north-west Anglesey and the Skerries, with the locations of the tidal turbines highlighted. The location of the farm is chosen based on two factors, i.e. acceptable water depth and large flow rate. The turbine farm is located in the middle of the waterway to minimize its impacts on local shores. The farm consists of 18 turbines, with each represented by an individual mesh cell of 15-20 m in size. Vertically, the turbines are located at the mid-depth. The turbines in the farm are aligned in a staggered way. They are separated from each other by 8D laterally and 15D in the up/downstream flow direction.

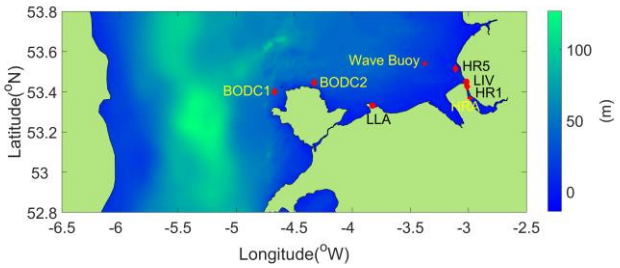

Fig. 3. Bathymetry of the model and locations of validation datasets. Circles are locations of tide gauges; Diamonds are where tidal current data was collected; Star denotes the location of the WaveNet Buoy; Cross indicates where suspended sediment concentration was measured.

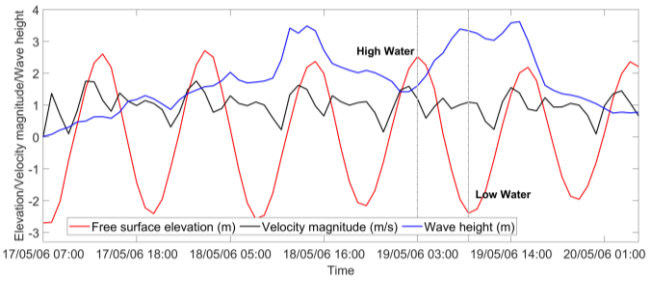

Fig. 4. Model calculated free surface elevation, depth-averaged velocity and wave height at the turbine farm location from 17/05/2006 07:00:00am to 20/05/2006 05:00:00am. During this time period, wave height peaks at 3.62 m at the selected farm location, representing moderate wave to stormy wave conditions.

III. Results

A. Model validation

1) Tidal level

The model predicted tidal water level is calibrated against measurements at two gauges provided by the UK Tide Gauge Network located within the study domain (LLA and LIV in Fig. 3). The free surface elevation comparison presented in Fig. 6 shows 750-hour results from the total model running period. To quantify the difference, harmonic analysis is carried out at both sites. In total, 29 tidal constituents are recognized by the analysis and M_2 and S_2 are suggested as the dominant constituents. Tables I and II compare the model predicted tidal harmonic constants of M_2 and S_2 with those measured on-site. The model results agree very well with the observations for both amplitude and phase at both sites. Discrepancy between model predicted and measured amplitude is within 4.5% at site LLA and 8.1% at site LIV. The model predicted tidal amplitudes and angles are slightly smaller than those measured on-site, suggesting that the high tide in the model arrives ahead of that obtained in the observation. However, the phase difference is within 3 minutes. These differences could be due to the uncertainties in the bottom bathymetry at the gauge sites. Overall, the model is able to provide accurate predictions of tidal elevation within the study domain.

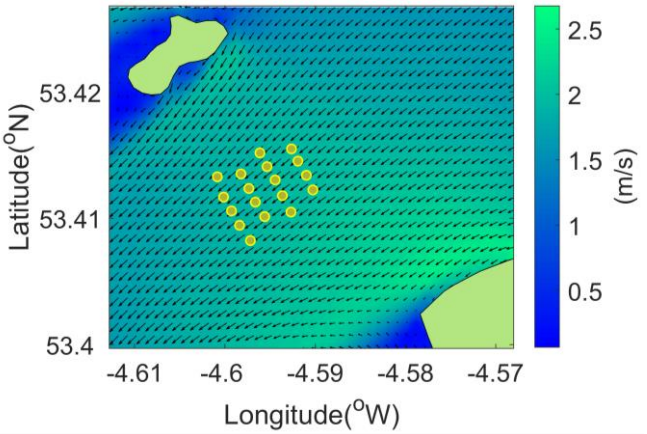

Fig. 5. A typical pattern of water depth averaged velocity between the north-west Anglesey and the Skerries, with arrows indicating flow directions. Locations of turbines are depicted by circles. They are separated from each other by 8D laterally and 15D in the up/downstream flow direction.

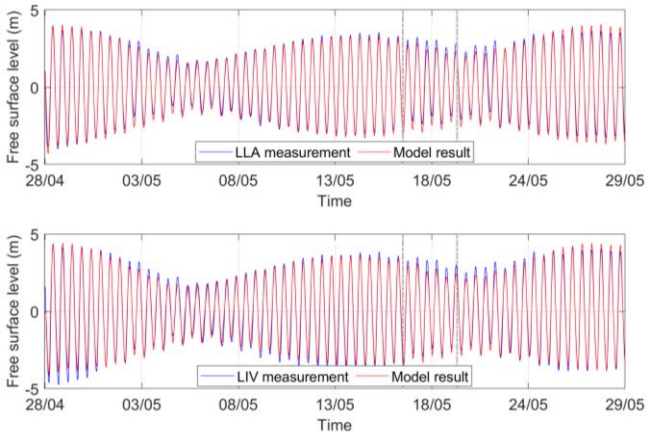

Fig. 6. Comparison of free surface elevation at the two tide gauge sites. The dot-dashed lines indicate the start (17/05/2006 07:00:00am) and the end (20/05/2006 05:00:00am) of the model run for the case with turbines.

2) Tidal current

To examine the reliability of the model in predicting tidal current, model predicted velocities at the sea surface, mid-depth and bottom layers are compared with two measured data sources. These two data sources are: (1) Measurements taken by HR Wallingford during the 1983 Mersey Barrage study [28]. Data measured at two sites (HR1 and HR5 in Fig. 3) is used for validation in the present research. (2) Current meter data downloaded from the British Oceanographic Data Centre (BODC). The BODC current meter data archive was obtained through a number of projects covering a large area as well as a long time span. Vertical coverage of this data source varies among datasets. Data collected at two sites (BODC1 and BODC2 in Fig. 3) off the coast of the Anglesey island is used in the present research to assess the reliability of the model in predicting tidal current. These two datasets date back to years 1970 and 1982, respectively.

Table III gives a brief summary of the tidal current validation data. Data availability along the water depth varies among these sites. For example, tidal current was measured at three depths at site HR1 whereas it was only measured very close to the bottom at site BODC2.

Fig. 7 and Fig. 8 present the model computed tidal current velocities against HR Wallingford measured data at locations HR1 and HR5. Model predictions and field measurements agree very well at three depths at site HR1. Predicted peak velocities during flood and ebb tides are close to the field measurements. A noticeable feature of the current at site HR1, i.e. rapid increase and prolonged decrease of flow speed during flood tide and, conversely, prolonged increase and sharp decrease of flow speed during ebb tide, is also being simulated correctly by the model. The performance of the model at site HR5, however, is less accurate. Peak velocity during flood tide is over-estimated and it is largely under-estimated during ebb tide. These discrepancies could be attributed to uncertainties of the bathymetry used in the model.

Fig. 9 and Fig. 10 show the performance of the model at the two BODC measuring sites. In general, the result is in good agreement with the measurements. Peak velocity is slightly under-estimated during both flood and ebb tides at site BODC1. The model clearly shows a very good agreement with the measurements at site BODC2. In general, performance of the model in simulating three-dimensional flow structure is satisfactory.

3) Surface waves

The computed significant wave height and wave direction are validated against data collected by a WaveNet buoy (Wave Buoy in Fig. 3). Fig. 11 presents the modelled wave height and direction of 750-hour results against the WaveNet buoy data which has a missing data gap between 05/05/2006 and 08/05/2006. In general, the model is capable of predicting the magnitude and phase changes of wave height and direction, even for the large storms around 01/05/2006, 18/05/2006 and 24/05/2006.

TABLE I
TIDAL HARMONIC ANALYSIS COMPARISON FOR M_2 CONSTITUENT

Site name	Observations		FVCOM	
	H_n (m)	φ_n (°)	H_n (m)	φ_n (°)
LIV	3.08	320.12	3.00	318.78
LLA	2.72	309.83	2.83	309.32

TABLE II
TIDAL HARMONIC ANALYSIS COMPARISON FOR S_2 CONSTITUENT

Site name	Observations		FVCOM	
	H_n (m)	φ_n (°)	H_n (m)	φ_n (°)
LIV	0.92	345.05	0.88	344.08
LLA	0.83	332.07	0.83	331.35

TABLE III
A BRIEF SUMMARY OF THE TIDAL CURRENT VALIDATION DATA

Site name		Time	Surface	Mid-depth	Bottom
HR	1	1983	Yes	Yes	Yes
	5	1983	Yes	No	Yes
BODC	1	1970	No	10/35	30/35
	2	1982	No	No	35/38

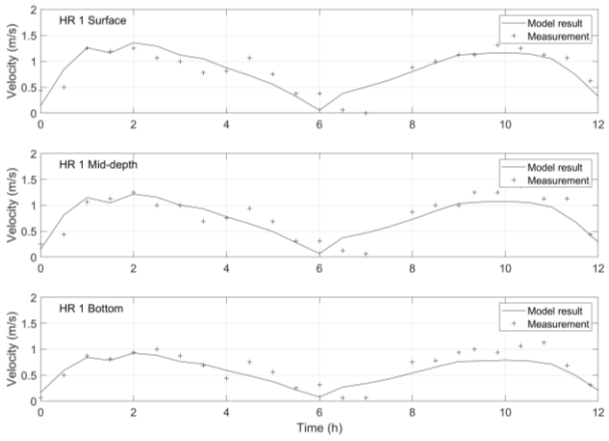

Fig. 7. Comparison of model predicted and measured flow velocity at three levels at HR1.

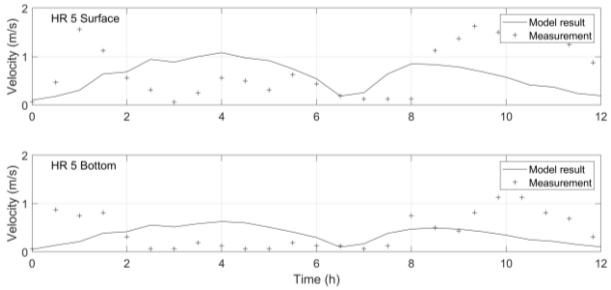

Fig. 8. Comparison of model predicted and measured flow velocity at two levels at HR5.

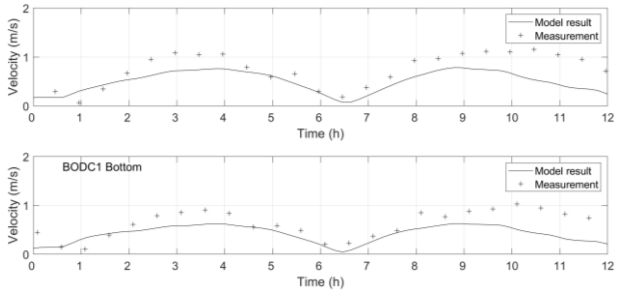

Fig. 9. Comparison of model predicted and measured flow velocity at two levels at BODC1.

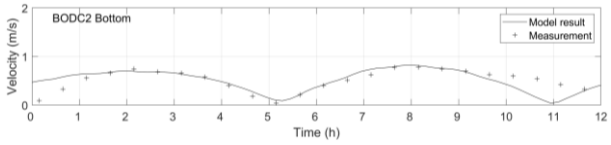

Fig. 10. Comparison of model predicted and measured flow velocity at bottom at BODC2.

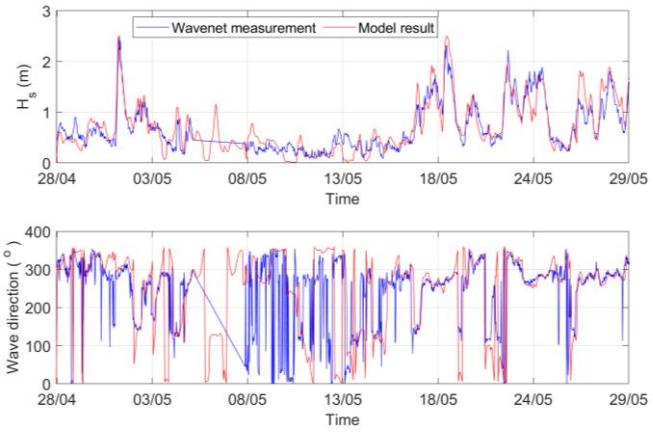

Fig. 11. Comparison of model significant wave height and wave direction against measurements over a month.

B. *Model application*

Through comparing the results of the cases with and without turbines, this section aims to explore the interactions between the turbine farm and its surrounding environment.

1) *Surface elevation*

The results in this section show free surface elevation changes in the Anglesey coast area at High Water (HW) indicated in Fig. 4 as a result of the inclusion of the turbine farm. It can be seen from Fig. 12 that at HW, the current flows towards the south-west, and the surface elevation around the farm site reduces by up to ~ 10 mm. The reduction continues to be observed west of the Skerries. Two eddies are observed - one slightly south-west of the farm and another one off the west coast of Holy island. Elevation decrease is seen at the centres of these two eddies. Increase of elevation can be seen downstream and further upstream of the device farm, as well as within the Cymyran strait separating Holy island from Anglesey.

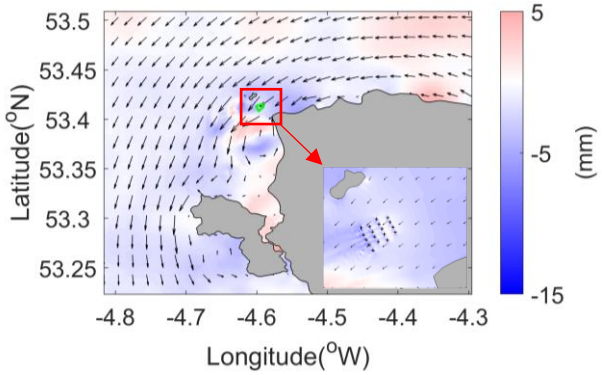

Fig. 12. Surface elevation change at High Water (HW). Arrows are imposed to indicate the flow direction.

2) *Flow field*

Fig. 13 shows changes caused by the turbine farm in flow fields at the surface, the mid-layer and the bottom as well as depth-averaged flow fields at HW, when the current is flowing towards the south-west. A strong jet of decelerated flow downstream of the farm is observed at the surface layer, sandwiched by two jets of accelerated flow, suggesting that the flow is diverted due to the blockage effect of the farm. The accelerated flow jets are also observed in the depth-averaged flow field. They are however much less visible at the mid-layer and the bottom. The mid-layer shows the maximum decrease of water velocity because the turbines are located at mid-depth, hence the maximum energy loss. The affected area in terms of water velocity is consistent throughout the water depth and, unlike surface elevation, it mainly follows the flow direction. The magenta lines in Fig. 15D delineate boundaries beyond which velocity recovery is larger than 95%, hence the limit of the wake. The length of the wake is ~ 9.0 km (~ 450D, i.e. ~ 14 times the width of the turbine farm). Similar results are shown in Fairley et al. [29] for a study of an array in the Pentland Firth.

Locally (insets of Fig. 13), the wake of each turbine can be clearly seen. It is also found that, in the vicinity of the turbine farm, although the surface and the mid-layer mainly experience flow deceleration, and the depth averaged flow fields suggest overall decelerated flow in the wake, the water at the bottom is accelerated, indicating that, vertically, the decelerated water due to the blockage of the farm squeezes its way through the bottom layers, which could lead to increased bottom shear stress.

3) *TKE*

Fig. 14 shows changes in TKE at the surface, the mid-layer and the bottom at HW. It can be seen from the figure that the impact of the turbines on TKE is restricted to the local area of the device farm. The presence of the turbine farm increases local TKE around the devices from nearly 0

to 0.09 m^2/s^2 at the mid-layer. The wake of each turbine in terms of TKE change stretches up to a distance of approximately 15D and the farm as a whole does not extend the length any longer. Compared to the mid-layer, TKE enhancement at the other two layers is less significant, but detectable.

4) Surface waves

Fig. 15 shows changes in significant wave height of surface waves at HW. It can be seen from the figure that an area is affected by the implementation of the turbines, even though the effect is small outside the vicinity of the farm. At HW, when the current is flowing towards the south-west, the effect at regional scale is mainly a reduction of wave height of 0.02-0.09 m in the vicinity and downstream of the farm. Wave height in the upstream region is also slightly reduced.

5) Bed shear stress

Fig. 16 shows changes in bed shear stress at HW. It can be seen from the figure that the presence of the turbine farm affects the bed shear stress of a large area. This is because the calculation of bottom shear stress depends highly on flow velocity and wave height, both of which experience regional changes due to the implementation of the turbine farm. Bed shear stress in the vicinity of the turbine farm is enhanced by up to 2.5 N/m^2. Bed shear stress outside the turbine farm, on the other hand, is reduced by ~ 0.3 N/m^2. This pattern agrees with that of the flow field.

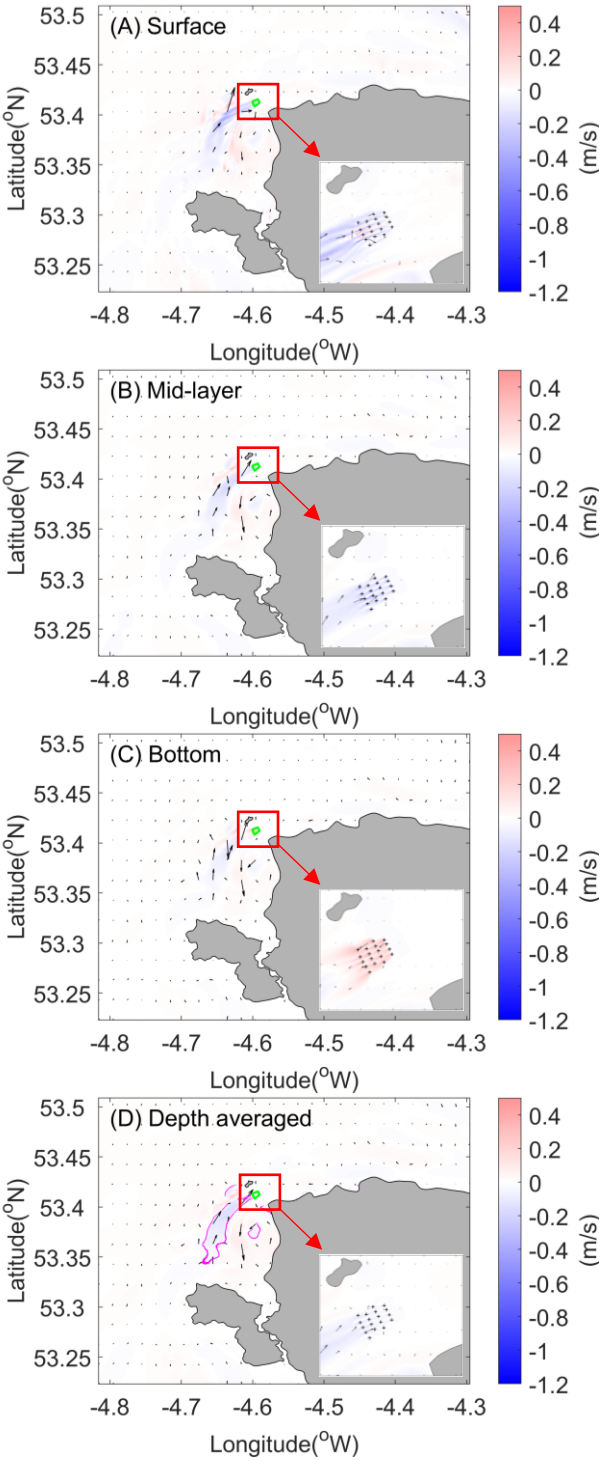

Fig. 13. Changes of flow fields at HW.

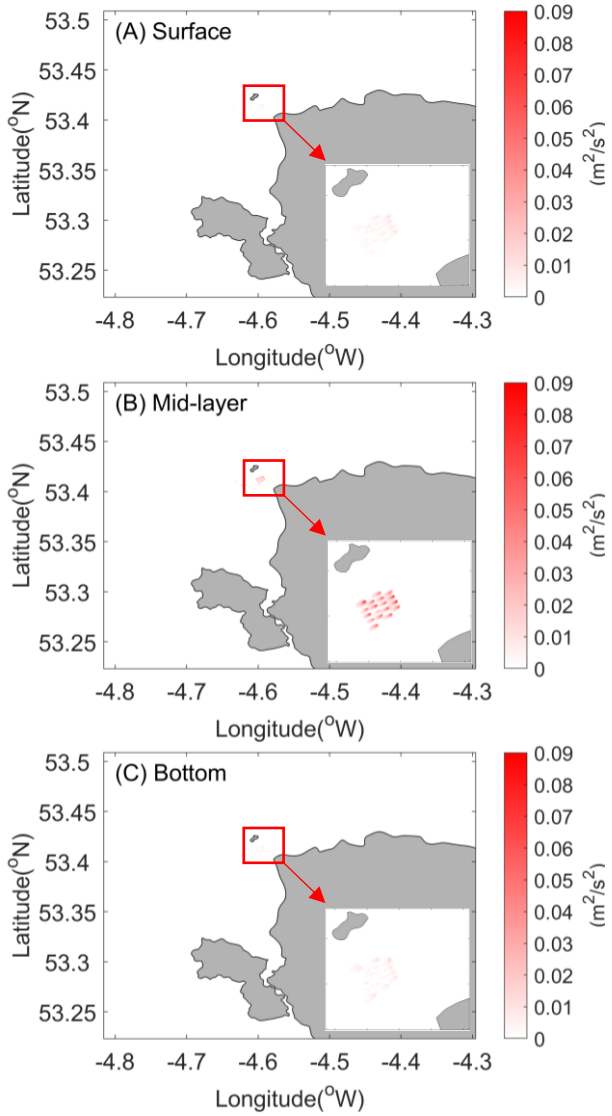

Fig. 14. Changes of TKE at HW.

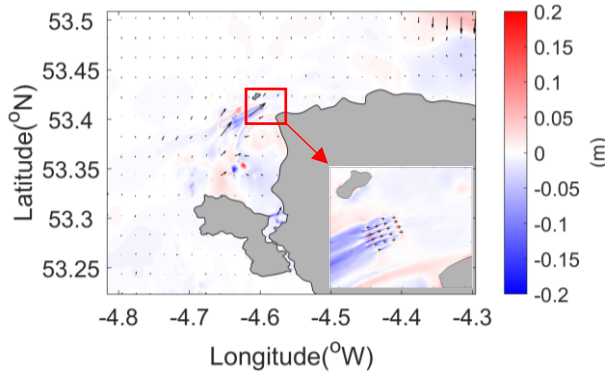

Fig. 15. Changes of significant wave height of surface waves at HW.

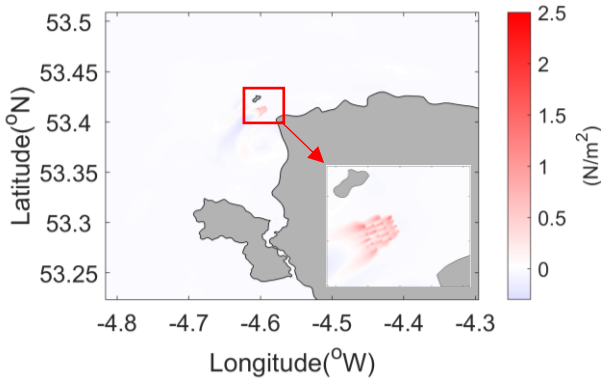

Fig. 16. Changes of bed shear stress at HW.

IV. Conclusions

In this research, a high spatial resolution, three-dimensional model is created for a region of the Irish Sea using FVCOM. The hydrodynamics, including tidal elevation, tidal current and surface waves, are validated against field measurements.

To study the interactions between a turbine farm comprised of 18 turbines and the surrounding environment, modifications made by the authors to the current, turbulence and surface wave modules of FVCOM for simulating turbines are used. With a definition of wake edge as 95% flow rate recovery, our results indicate that there are slight wake effects for a distance of around 14 times the array width downstream of the device farm. Wake recovery, however, was found to be sensitive to turbulence intensity (e.g. ref. [11]). Sensitivity of wake length to the turbulence closure, therefore, remains an interesting avenue of research. As a result of high spatial resolution used, local effects of the turbine farm are revealed by the model. These include flow acceleration on both sides of the turbine farm, flow acceleration near the bed in the vicinity of the turbine farm which leads to enhanced bed shear stress, and locally increased TKE. Apart from these strong local effects, the turbine farm is also found to have impact on the regional hydrodynamics and surface waves although these regional scale impacts are much less prominent than the local effects (e.g. bed shear stress reduction of ~ 0.3 N/m² outside the turbine farm, in contrast to bed shear stress enhancement of 2.5 N/m² in the vicinity of the turbine farm).

In terms of future research, the validated Irish Sea model aims to provide boundary conditions for high-resolution CFD models focused on individual development sites within the West Anglesey Demonstration Zone. Comparison between wake behaviours and performance of turbine arrays produced by the FVCOM (as a representative of large scale coastal area models) and CFD models will be carried out to explore the strengths and weaknesses of each model.

References

[1] Department for Business, Energy and Industrial Strategy, "Energy innovation needs assessment. sub-theme report: Tidal stream. Technical report," 2019. [Online]. Available:

https://assets.publishing.service.gov.uk/government/uploads/system/uploads/attachment_data/file/845665/energy-innovation-needs-assessment-tidal-stream.pdf

[2] G. Smart, and M. Noonan, "Tidal stream and wave energy cost reduction and industrial benefit," 2018. [Online]. Available: https://www.marineenergywales.co.uk/wp-content/uploads/2018/05/ORE-Catapult-Tidal-Stream-and-Wave-Energy-Cost-Reduction-and-Ind-Benefit-FINAL-v03.02.pdf

[3] A. Bahaj, L. Myers, M. Thomson, and N. Jorge, "Characterising the wake of horizontal axis marine current turbines," In *Proceedings of the 7th European Wave and Tidal Energy Conference, Port, Portugal, 11–14th September, 2007*.

[4] S. Tedds, I. Owen, and R. Poole, "Near-wake characteristics of a model horizontal axis tidal stream turbine," *Renewable Energy*, vol. 63, pp. 222–235, 2014.

[5] F. Maganga, G. Germain, J. King, G. Pinon, and E. Rivoalen, "Experimental characterisation of flow effects on marine current turbine behaviour and on its wake properties," *IET Renewable Power Generation*, vol. 4, pp. 498–509, 2010.

[6] A. Ortega, A. Nambiar, D. Ingram, and D. Sale, "Torque control of a laboratory scale variable speed hydrokinetic tidal turbine-CFD simulation and validation," In *Proceedings of the ASME 39th International Conference on Ocean, Offshore and Arctic Engineering, Fort Lauderdale, FL, USA, 2020.*

[7] T. de Jesus Henriques, S. Tedds, A. Botsari, G. Najafian, T. Hedges, C. Sutcliffe, I. Owen, and R. Poole, "The effects of wave–current interaction on the performance of a model horizontal axis tidal turbine," *International Journal of Marine Energy*, vol. 8, pp. 17–35, 2014.

[8] A. Mason-Jones, D. M. O'Doherty, C. E. Morris, T. O'Doherty, C. Byrne, P. W. Prickett, R. I. Grosvenor, I. Owen, S. Tedds, and R. Poole, "Non-dimensional scaling of tidal stream turbines," *Energy*, vol. 44, pp. 820–829, 2012.

[9] R. Malki, A. Williams, T. Croft, M. Togneri, and I. Masters, "A coupled blade element momentum–Computational fluid dynamics model for evaluating tidal stream turbine performance," *Applied Mathematical Modelling*, vol. 37, pp. 3006–3020, 2013.

[10] M. Edmunds, A. J. Williams, I. Masters, A. Banerjee, and J. H. VanZwieten, "A spatially nonlinear generalised actuator disk model for the simulation of horizontal axis wind and tidal turbines," *Energy*, vol. 194, pp. 116803, 2020.

[11] M. Edmunds, A. J. Williams, I. Masters, and T. Croft, "An enhanced disk averaged CFD model for the simulation of horizontal axis tidal turbines," *Renewable Energy*, vol. 101, pp. 67–81, 2017.

[12] D. D. Apsley, T. Stallard, and P. K. Stansby, "Actuator-line CFD modelling of tidal-stream turbines in arrays," *Journal of Ocean Engineering and Marine Energy*, vol. 4, pp. 259–271, 2018.

[13] R. Martin-Short, J. Hill, S. Kramer, A. Avdis, P. Allison, and M. Piggott, "Tidal resource extraction in the Pentland Firth, UK: Potential impacts on flow regime and sediment transport in the Inner Sound of Stroma," *Renewable Energy*, vol. 76, pp. 596–607, 2015.

[14] J. Thiébot, P. B. du Bois, and S. Guillou, "Numerical modeling of the effect of tidal stream turbines on the hydrodynamics and the sediment transport–application to the Alderney Race (Raz Blanchard), France," *Renewable Energy*, vol. 75, pp. 356–365, 2015.

[15] Z. Defne, K. A. Haas, and H. M. Fritz, "Numerical modeling of tidal currents and the effects of power extraction on estuarine hydrodynamics along the Georgia coast, USA," *Renewable Energy*, vol. 36, pp. 3461–3471, 2011.

[16] Z. Yang, T. Wang, and A. E. Copping, "Modeling tidal stream energy extraction and its effects on transport processes in a tidal channel and bay system using a three-dimensional coastal ocean model," *Renewable Energy*, vol. 50, pp. 605–613, 2013.

[17] D. Fallon, M. Hartnett, A. Olbert, and S. Nash, "The effects of array configuration on the hydro-environmental impacts of tidal turbines," *Renewable Energy*, vol. 64, pp. 10–25, 2014.

[18] Brown, A. J. G., Neill, S. P., & Lewis, M. J. (2017). Tidal energy extraction in three-dimensional ocean models. *Renewable Energy*, vol. 114, pp. 244-257.

[19] T. Roc, D. C. Conley, and D. Greaves, "Methodology for tidal turbine representation in ocean circulation model," *Renewable Energy*, vol. 51, pp. 448–464, 2013.

[20] X. Li, M. Li, S. J. McLelland, L.-B. Jordan, S. M. Simmons, L. O. Amoudry, R. Ramirez-Mendoza, and P. D. Thorne, "Modelling tidal stream turbines in a three-dimensional wave-current fully coupled oceanographic model," *Renewable Energy*, vol. 114, pp. 297–307, 2017.

[21] X. Li, M. Li, L.-B. Jordan, S. McLelland, D. R. Parsons, L. O. Amoudry, Q. Song, and L. Comerford, "Modelling impacts of tidal stream turbines on surface waves," *Renewable energy*, vol. 130, pp. 725–734, 2019.

[22] X. Li, M. Li, L. O. Amoudry, R. Ramirez-Mendoza, P. D. Thorne, Q. Song, P. Zheng, S. M. Simmons, L.-B. Jordan, and S. J. McLelland, "Three-dimensional modelling of suspended sediment transport in the far wake of tidal stream turbines," *Renewable Energy*, vol. 151, pp. 956–965, 2020.

[23] M. Dobson, W. Evans, K. James, "The sediment on the floor of the southern Irish Sea," *Marine Geology*, vol. 11, pp. 27-69, 1971.

[24] Black & Veatch, "Phase II UK Tidal Stream Energy Resource Assessment, A report to the Carbon Trust's Marine Energy Challenge," 2005.

[25] Marine Energy Wales, "West Anglesey Tidal Demonstration Zone". [Online]. Available: https://www.marineenergywales.co.uk/marine-energy-in-wales/demonstration-zones/anglesey-demonstration-zone/.

[26] Piano, M., Ward, S., Robins, P., Neill, S., Lewis, M., Davies, A., Powell, B., Owen, A.W. and Hashemi, R., 2015. Characterizing the tidal energy resource of the West Anglesey Demonstration Zone (UK), using Telemac-2D and field observations. *In Proceedings of the XXII TELEMAC-MASCARET Technical User Conference October 15-16, 2015* (pp. 195-203).

[27] R. Burrows, I. A. Walkington, N. C. Yates, T. S. Hedges, J. Wolf, and J. Holt, "The tidal range energy potential of the West Coast of the United Kingdom," *Applied Ocean Research*, vol. 31, pp. 229-238, 2009.

[28] H. Wallingford, "Mersey barrage feasibility study: stage iiia, 3d mathematical modelling of tidal flows and sedimentation. Technical report," 1992.

[29] I. Fairley, I. Masters, and H. Karunarathna, "The cumulative impact of tidal stream turbine arrays on sediment transport in the Pentland Firth," *Renewable Energy*, vol. 80, pp. 755-769, 2015.